J|A|C|S
ARTICLES
Published on Web 01/11/2006

pH Rate Profiles of F_nY_{356}−R2s ($n = 2, 3, 4$) in *Escherichia coli* Ribonucleotide Reductase: Evidence that Y_{356} Is a Redox-Active Amino Acid along the Radical Propagation Pathway

Mohammad R. Seyedsayamdost, Cyril S. Yee, Steven Y. Reece, Daniel G. Nocera,* and JoAnne Stubbe*

Contribution from the Department of Chemistry, Massachusetts Institute of Technology, 77 Massachusetts Avenue, Cambridge, Massachusetts 02139-4307

Received August 28, 2005; E-mail: nocera@mit.edu; stubbe@mit.edu

Abstract: The *Escherichia coli* ribonucleotide reductase (RNR), composed of two subunits (R1 and R2), catalyzes the conversion of nucleotides to deoxynucleotides. Substrate reduction requires that a tyrosyl radical (Y_{122}•) in R2 generate a transient cysteinyl radical (C_{439}•) in R1 through a pathway thought to involve amino acid radical intermediates [Y_{122}• → W_{48} → Y_{356} within R2 to Y_{731} → Y_{730} → C_{439} within R1]. To study this radical propagation process, we have synthesized R2 semisynthetically using intein technology and replaced Y_{356} with a variety of fluorinated tyrosine analogues (2,3-F_2Y, 3,5-F_2Y, 2,3,5-F_3Y, 2,3,6-F_3Y, and F_4Y) that have been described and characterized in the accompanying paper. These fluorinated tyrosine derivatives have potentials that vary from −50 to +270 mV relative to tyrosine over the accessible pH range for RNR and pK_as that range from 5.6 to 7.8. The pH rate profiles of deoxynucleotide production by these F_nY_{356}−R2s are reported. The results suggest that the rate-determining step can be changed from a physical step to the radical propagation step by altering the reduction potential of Y_{356}• using these analogues. As the difference in potential of the F_nY• relative to Y• becomes >80 mV, the activity of RNR becomes inhibited, and by 200 mV, RNR activity is no longer detectable. These studies support the model that Y_{356} is a redox-active amino acid on the radical-propagation pathway. On the basis of our previous studies with 3-NO_2Y_{356}−R2, we assume that 2,3,5-F_3Y_{356}, 2,3,6-F_3Y_{356}, and F_4Y_{356}−R2s are all deprotonated at pH > 7.5. We show that they all efficiently initiate nucleotide reduction. If this assumption is correct, then a hydrogen-bonding pathway between W_{48} and Y_{356} of R2 and Y_{731} of R1 does not play a central role in triggering radical initiation nor is hydrogen-atom transfer between these residues obligatory for radical propagation.

Introduction

Class I *Escherichia coli* ribonucleotide reductase (RNR) plays a crucial role in DNA replication and repair by catalyzing the reduction of nucleoside diphosphates (NDPs) to deoxynucleoside diphosphates (dNDPs).[1,2] It is composed of two homodimeric subunits, designated R1 and R2. A complex between R1 and R2 is required for activity.[3] R1 houses the NDP binding sites and the binding sites for the effectors that control the specificity and rate of nucleotide reduction.[3−5] R2 harbors the diferric tyrosyl radical (Y_{122}•) cofactor proposed to initiate nucleotide reduction by generating a transient thiyl radical (C_{439}•) in the active site of R1.[6] The crystal structures of both R1 and R2 have been solved independently.[7−9] A docking model of the two proteins has been generated using these structures on the basis of their shape complementarity and on knowledge of conserved residues.[7] This model, a 1:1 complex of the R1 and R2 homodimers, places the Y_{122}• on R2 at a distance >35 Å away from the terminal site of oxidation on R1, the C_{439} residue. Electron tunneling between these residues according to Marcus theory ($k_{ET} = 10^{-6}$ s^{-1} for $\beta = 1.2$ Å^{-1} under activationless conditions) is too slow to account for a k_{cat} of ∼2−10 s^{-1}.[10] Thus, the radical generation process has been proposed to occur via a hopping mechanism involving aromatic amino acid radical intermediates, as shown in Figure 1.[7,11] Mounting evidence is calling into question the symmetry of the docking model.[12,13] However, a strong case can be made for involvement of the residues on this pathway, specifically Y_{356} on R2 and Y_{731} and Y_{730} on R1. They are the only absolutely conserved residues

(1) Jordan, A.; Reichard, P. *Annu. Rev. Biochem.* **1998**, *67*, 71.
(2) Stubbe, J.; van der Donk, W. A. *Chem. Rev.* **1998**, *98*, 705.
(3) Thelander, L. *J. Biol. Chem.* **1973**, *248*, 4591.
(4) Kashlan, O. B.; Scott, C. P.; Lear, J, D.; Cooperman, B. S. *Biochemistry* **2002**, *41*, 462.
(5) Kashlan, O. B.; Cooperman, B. S. *Biochemistry* **2003**, *42*, 1696.
(6) Stubbe, J.; Riggs-Gelasco, P. *Trends Biochem. Sci.* **1998**, *23*, 438.
(7) Uhlin, U.; Eklund, H. *Nature* **1994**, *370*, 533.
(8) Nordlund, P.; Sjöberg, B.-M.; Eklund, H. *Nature* **1990**, *345*, 593.
(9) Högbom, M.; Galander, M.; Andersson, M.; Kolberg, M.; Hofbauer, W.; Lassmann, G.; Nordlund, P.; Lendzian, F. *Proc. Natl. Acad. Sci. U.S.A.* **2003**, *100*, 3209.
(10) Marcus, R. A.; Sutin, N. *Biochim. Biophys. Acta* **1985**, *811*, 265.
(11) Stubbe, J.; Nocera, D. G.; Yee, C. S.; Chang, M. C. Y. *Chem. Rev.* **2003**, *103*, 2167.
(12) Erickson, H. K. *Biochemistry* **2001**, *40*, 9631.
(13) Ge, J.; Yu, G.; Ator, M. A.; Stubbe, J. *Biochemistry* **2003**, *42*, 10071.

10.1021/ja055927j CCC: $33.50

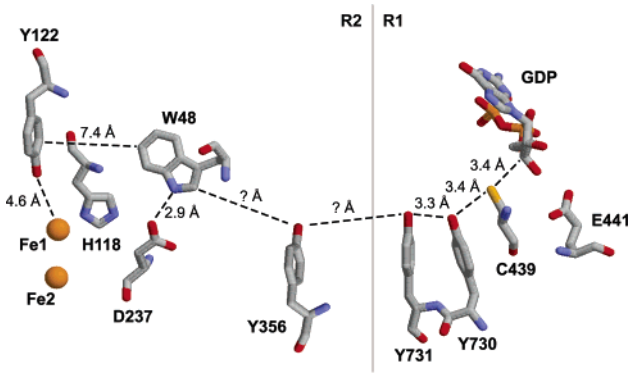

Figure 1. Putative PCET pathway of *E. coli* RNR based on the docking model in ref 7. Y_{356} is not visible in the crystal structure of R2; it is proposed to propagate the radical between W_{48} on R2 and Y_{731} on R1. Distances on the R2 side are taken from the crystal structure of oxidized R2 at 1.4 Å resolution, given in ref 9.

that are not involved in assembly of the di-iron cofactor or in the nucleotide-reduction process.[13,14]

Efforts to examine this pathway model experimentally and identify the mechanism(s) for radical propagation have heretofore relied on site-directed mutagenesis of each amino acid within the pathway on both the *E. coli* and mouse RNRs.[15−18] More recently, in vivo complementation studies in *E. coli* using pathway mutants to investigate radical migration have been reported.[19] These studies demonstrate the requirement for these residues (Figure 1) in nucleotide reduction. However, they are not amenable to addressing the mechanism of the radical propagation process or the intermediacy of amino acid radicals as the proteins are "inactive". Investigation of the radical propagation process is further complicated by results from steady-state and pre-steady-state kinetic analyses of *E. coli* RNR, which suggest that radical propagation and nucleotide reduction are preceded by a slow physical step and that binding of substrate and effector trigger this physical step.[13] This conformational gating makes the electron transfer (ET) step kinetically invisible and, thus, impossible to study. One way to gain insight into the propagation reaction, therefore, is to change the rate-limiting step from this physical step to ET by altering the reduction potential of a residue within the pathway.

The limited repertoire of natural amino acids does not allow for an informative perturbation to be made and thus we have recently turned to site-specific insertions of unnatural amino acids into R2 at Y_{356} using protein-ligation methods.[20] A 3-NO_2Y_{356}−R2 construct has allowed us to measure the pK_a of a single amino acid residue in a putative 260 kDa R1/R2 complex.[21] A 2,3-F_2Y_{356}−R2 provided the first clues that the phenolic proton at 356 in R2 is not required for conformational gating of turnover.[22] Results from studying the aniline amino acid, $Y_{356}PheNH_2$−R2 construct,[23] suggested that the rate of radical transfer through position 356 is affected mainly by the reduction potential of the residue at that position and not controlled by hydrogen bonding or proton transfer. To assess the interplay between the electron- and proton-transfer events requires the systematic variation of the radical-reduction potential and phenolic pK_a at Y_{356}, the proposed gate keeper for radical transport between the R1 and R2 subunits. In the accompanying paper,[24] we reported the synthesis and characterization of a number of unnatural *N*-acetyl and *C*-amide protected fluorotyrosine analogues, Ac−F_nY−NH_2, (Table 1). These derivatives have radical peak-reduction potentials that vary from −50 to +270 mV relative to Ac−Y•−NH_2 in the pH region in which RNR activity can be measured and pK_as that range from 5.6 to 7.8. We suggested that these analogues would be useful in probing the mechanism(s) of proton coupled electron transfer (PCET) in systems that involve redox-active tyrosines.

Table 1. Fluorotyrosine Derivatives Used To Substitute Y_{356} of R2 and Their Physical Properties

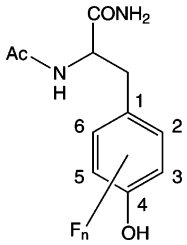

fluorotyrosine	pK_a	E_p(Y•/Y⁻)/ mV
Ac−Y−NH_2	9.9	642
Ac−3,5-F_2Y−NH_2	7.2	755
Ac−2,3-F_2Y−NH_2	7.8	810
Ac−2,3,5-F_3Y−NH_2	6.4	853
Ac−2,3,6-F_3Y−NH_2	7.0	911
Ac−F_4Y−NH_2	5.6	968

We now report the semisynthesis of R2, in which Y_{356} has been replaced with fluorinated tyrosine derivatives of Table 1. These R2 analogues have allowed us to study the role of Y_{356} in the radical-propagation process of *E. coli* RNR. The results suggest that an increase in the peak-reduction potential of the F_nY analogue relative to Y by 80 mV results in a change in the rate-limiting step from a conformational change to the radical propagation process. These studies support the proposal that the protonation state of the phenol of this residue is not important in conformational gating, that the proton can be lost from this pathway without affecting the overall enzymatic activity, and that Y_{356} is a redox-active amino acid on the radical propagation pathway. Additionally, the rigorous assessment of the enzymatic activity afforded by the F_nY_{356}−R2 series establishes that the energetics of radical hopping through Y_{356} is finely tuned in wild-type (wt) class I RNR and can only operate within a ∼150 mV window for the Y•/Y redox couple.

Materials and Methods

Materials. ATP, cytidine-5'-diphosphate (CDP), reduced β-nicotinamide adenine dinucleotide phosphate (NADPH), *N*-hydroxyurea, trifluoroacetic acid (TFA), 2-mercaptoethanesulfonic acid (MESNA),

(14) Eklund, H.; Uhlin, U.; Farnegardh, M.; Logan, D. T.; Nordlund, P. *Prog. Biophys. Mol. Biol.* **2001**, *77*, 177.
(15) Ekberg, M.; Sahlin, M.; Eriksson, M.; Sjöberg, B. M. *J. Biol. Chem.* **1996**, *271*, 20655.
(16) Ekberg, M.; Potsch, S.; Sandin, E.; Thunnissen, M.; Nordlund, P.; Sahlin, M.; Sjöberg, B. M. *J. Biol. Chem.* **1998**, *273*, 21003.
(17) Rova, U.; Goodtzova, K.; Ingemarson, R.; Behravan, G.; Gräslund, A.; Thelander, L. *Biochemistry* **1995**, *34*, 4267.
(18) Rova, U.; Adrait, A.; Potsch, S.; Gräslund, A.; Thelander, L. *J. Biol. Chem.* **1999**, *274*, 23746.
(19) Ekberg, M.; Birgander, P.; Sjöberg, B.-M. *J. Bacteriol.* **2003**, *185*, 1167.
(20) Muir, T. W. *Annu. Rev. Biochem.* **2003**, *72*, 249.
(21) Yee, C. S.; Seyedsayamdost, M. R.; Chang, M. C.; Nocera, D. G.; Stubbe, J. *Biochemistry* **2003**, *42*, 14541.
(22) Yee, C. S.; Chang, M. C.; Ge, J.; Nocera, D. G.; Stubbe, J. *J. Am. Chem. Soc.* **2003**, *125*, 10506.
(23) Chang, M. C. Y.; Yee, C. S.; Nocera, D. G.; Stubbe, J. *J. Am. Chem. Soc.* **2004**, *126*, 16702.
(24) Seyedsayamdost, M. R.; Reece, S. Y.; Nocera, D. G.; Stubbe, J. A. *J. Am. Chem. Soc.* See accompanying paper.

Fmoc-succinimide, Sephadex G-25 resin, DNase I (10 units/μL), and Triton X-100 were purchased from Sigma. BL21 (DE3) RIL Codon+ competent cells were obtained from Stratagene. Calf-intestine alkaline phosphatase (20 units/μL) was purchased from Roche. All amino acid derivatives were purchased from Novabiochem, Fmoc-L-Leu-PEG-PS resin and all other chemicals required for peptide synthesis were obtained from Applied Biosystems. [2-^{14}C]-CDP was purchased from Moravek Biochemicals. *E. coli* thioredoxin (TR, SA of 40 units/mg) and *E. coli* thioredoxin reductase (TRR, SA of 1800 units/mg) were isolated as previously described.[13]

Physical Measurements. ^{1}H NMR spectra were recorded on a Varian 300 MHz NMR spectrometer at the MIT Department of Chemistry Instrumentation Facility. NMR samples were internally referenced to tetramethylsilane. pH measurements were performed with an Orion microelectrode. Absorption spectra were recorded on an Agilent 8453 Diode Array spectrophotometer. EPR spectra were recorded at 77 K on a Bruker ESP-300 X-band (9.4 GHz) spectrometer equipped with an Oxford liquid helium cryostat.

Synthesis of Fmoc-F$_n$Ys. Fmoc-F$_n$Ys were synthesized by the method of Lapatsanis et al. with minor modifications.[25] The tyrosine analogue (700 μmol) was dissolved in 2.4 mL of 10% Na_2CO_3 and mixed with Fmoc-succinimide (970 μmol) in 2.5 mL of dioxane at 4 °C. The reaction was warmed to room temperature and reacted for 20 min to 2 h (F$_n$Ys with higher fluorine substitution required longer reaction times). The reaction was monitored via TLC using 10:1 $CHCl_3$/MeOH as the mobile phase. After completion, the reaction was quenched with 25 mL of water and extracted twice with 10 mL of EtOAc to remove Fmoc-succinimide. The pH was then lowered to 2−3 with 2 N HCl, and the solution was extracted with EtOAc (10×, 10 mL). The organic layer was washed with saturated NaCl (3×, 3 mL) and water (2×, 3 mL) and finally dried over $MgSO_4$. The solvent was removed in vacuo, and the product was purified by silica gel chromatography (16 g, 1.5 × 28 cm) using isocratic elution. The solvent system, R_f, and the yield for each analogue are summarized in Table S1 (Supporting Information).

Fmoc-L-3,5-F$_2$Y: ^{1}H NMR (300 MHz, CD_3OD) δ = 2.85 (dd, 1H, $C_\beta-H_1$, 9.7 Hz, 14.3 Hz), 3.12 (dd, 1H, $C_\beta-H_2$, 5.7 Hz, 14.3 Hz), 4.2 (m, 3H, fluorenyl C−H and $C-H_2$), 4.37 (dd, 1H, $C_\alpha-H$, 5.7 Hz, 10 Hz), 6.82 (m, 2H, PhOH C−H), 7.35 (dt, 4H, aromatic fluorenyl C−H, 7.6 Hz, 26.7 Hz), 7.62 (d, 2H, aromatic fluorenyl C−H, 7.5 Hz), 7.8 (d, 2H, aromatic fluorenyl C−H, 7.1 Hz).

Fmoc-L-2,3-F$_2$Y: ^{1}H NMR (300 MHz, CD_3OD) δ = 2.9 (dd, 1H, $C_\beta-H_1$, 9.6 Hz, 14.6 Hz), 3.23 (dd, 1H, $C_\beta-H_2$, 4.8 Hz, 14.2 Hz), 4.24 (m, 3H, fluorenyl C−H and $C-H_2$), 4.4 (dd, 1H, $C_\alpha-H$, 5 Hz, 9.7 Hz), 6.61 (m, 1H, PhOH $C-H_5$), 6.82 (m, 1H, PhOH $C-H_6$), 7.28 (m, 2H, aromatic fluorenyl C−H), 7.38 (t, 2H, aromatic fluorenyl C−H, 7.4 Hz), 7.6 (d, 2H, aromatic fluorenyl C−H, 7.4 Hz), 7.77 (d, 2H, aromatic fluorenyl C−H, 7.4 Hz).

Fmoc-L-2,3,6-F$_3$Y: ^{1}H NMR (300 MHz, CD_3OD) δ = 3.02 (dd, 1H, $C_\beta-H_1$, 9.3 Hz, 14 Hz), 3.2 (dd, 1H, $C_\beta-H_2$, 5.7 Hz, 13.9 Hz), 4.2 (m, 3H, fluorenyl C−H and $C-H_2$), 4.41 (dd, 1H, $C_\alpha-H$, 5.7 Hz, 9.4 Hz), 6.46 (m, 1H, PhOH C−H), 7.33 (dt, 4H, aromatic fluorenyl C−H, 7.1 Hz, 26.7 Hz), 7.6 (d, 2H, aromatic fluorenyl C−H, 7 Hz), 7.78 (d, 2H, aromatic fluorenyl C−H, 9 Hz).

Fmoc-L-2,3,5-F$_3$Y: ^{1}H NMR (300 MHz, CD_3OD) δ = 2.9 (dd, 1H, $C_\beta-H_1$, 9.6 Hz, 13.5 Hz), 3.25 (dd, 1H, $C_\beta-H_2$, 4.2 Hz, 13.8 Hz), 4.25 (m, 3H, fluorenyl C−H and $C-H_2$), 4.43 (dd, 1H, $C_\alpha-H$, 4.7 Hz, 9.2 Hz), 6.82 (m, 1H, PhOH C−H), 7.32 (dt, 4H, aromatic fluorenyl C−H, 7.2 Hz, 26.7 Hz), 7.58 (d, 2H, aromatic fluorenyl C−H, 7.2 Hz), 7.75 (d, 2H, aromatic fluorenyl C−H, 7.2 Hz).

Fmoc-L-2,3,5,6-F$_4$Y: ^{1}H NMR (300 MHz, CD_3OD) δ = 3.06 (dd, 1H, $C_\beta-H_1$, 9.2 Hz, 14.2 Hz), 3.26 (dd, 1H, $C_\beta-H_2$, 5.4 Hz, 14.2 Hz), 4.23 (m, 3H, nonaromatic fluorenyl−H), 4.38 (dd, 1H, $C_\alpha-H$, 5.4 Hz, 9.3 Hz), 7.34 (dt, 4H, aromatic fluorenyl−H, 7.7 Hz, 27 Hz), 7.61 (d, 2H, aromatic fluorenyl−H, 7.2 Hz), 7.78 (d, 2H, aromatic fluorenyl−H, 7.5 Hz).

Table 2. RP-HPLC and MALDI-TOF MS Characterization of F$_n$Y-22mers[a]

F$_n$Y-22mer	RP-HPLC R_t (min)	MS of (^{t}buthio)-protected F$_n$Y-22mer *m/z* [M − H]$^-$ calcd (obs)	MS of deprotected F$_n$Y-22mer *m/z* [M − H]$^-$ calcd (obs)
Y-22mer	19	2548.6 (2548.2)	2460.6 (2460.1)
2,3-F$_2$Y-22mer	19	2584.6 (2585.2)	2496.6 (2495.6)
3,5-F$_2$Y-22mer	18.5	2584.6 (2584.0)	2496.6 (2495.8)
2,3,6-F$_3$Y-22mer	19	2602.6 (2601.9)	2552.6 (2551.6)[c]
2,3,5-F$_3$Y-22mer	21.5	2602.6 (2601.5)	2552.6 (2551.6)[c]
F$_4$Y-22mer	18	2642.6 (2641.4)[b]	2570.6 (2570.3)[c]

[a] See ref 21 for detailed description of HPLC and MALDI-TOF methods. [b] [M − 2H + Na]$^-$. [c] [M − 2H + K]$^-$.

Table 3. Physical and Biochemical Characterization of F$_n$Y$_{356}$−R2s

F$_n$Y$_{356}$−R2	yield (mg)[a]	ESI-MS *m/z* [M + H]$^+$ calcd (obs)	radical content[b] (Y•/dimer)	maximal specific activity (nmol/min mg)[c]	K_m for R1 (μM)
Y−R2	14.3	43360 (43360)	0.34	450	0.55 ± 0.18
2,3-F$_2$Y$_{356}$−R2	15	43396 (43399)	0.33	370	0.62 ± 0.11
3,5-F$_2$Y$_{356}$−R2	20	43396 (43392)	0.31	450	nd[d]
2,3,5-F$_3$Y$_{356}$−R2	13	43414 (43410)	0.42	365	0.65 ± 0.15
2,3,6-F$_3$Y$_{356}$−R2	10.5	43414 (43413)	0.41	95	nd[d]
F$_4$Y$_{356}$−R2	10	43432 (43434)	0.42	30	0.59 ± 0.2
V$_{353}$G/ S$_{354}$C−R2[e]	−	−	1.1	1420	0.55 ± 0.21

[a] Amount recovered from incubation with 45 mg of MESNA-activated R2. [b] Measured by the dropline correction method and quantitative EPR methods using recombinant wt R2 as standard. [c] Activity of intein-generated F$_n$Y$_{356}$−R2s is normalized for radical content of Y−R2. [d] nd = not determined. [e] Made by recombinant methods.

Peptide Synthesis. The R2 C-terminal peptide CSF$_n$YLVGQIDSEVDTDDLSNFQL was synthesized by a combination of standard solid-phase and solution-phase peptide synthesis methods as previously described.[21] The first 19 residues were added using a Pioneer Peptide Synthesizer from Applied Biosystems. The remaining 3 amino acids (positions 20−22 on the peptide) were coupled manually. The manual coupling reaction of Fmoc-F$_n$Ys were carried out for 1 h, and a typical reaction contained 4 equiv of Fmoc-F$_n$Y, 3.6 equiv of O-(7-azabenzotriazole-1-yl)-*N*,*N*,*N*′,*N*′-tetramethyluronium hexafluorophosphate (HATU), and 8 equiv of diisopropyl ethylamine (DIPEA) in DMF. The purified peptides were characterized by RP-HPLC and MALDI-TOF MS. The results are summarized in Table 2.

Semisynthesis of R2 and F$_n$Y$_{356}$−R2s. Culture growth, ligation, and protein purification were carried out as previously described[21] with minor modifications. After MESNA-mediated cleavage of R2(1−353) from the chitin resin, excess MESNA was removed using a Sephadex G-25 column (200 mL, 3 cm × 30 cm) equilibrated in cleavage buffer (50 mM HEPES, pH 7.6, 500 mM NaCl). Furthermore, prior to purification by MonoQ anion exchange chromatography, unbound peptide was removed by concentration/dilution cycles using a YM-30 membrane. MonoQ purifications were performed under reducing conditions with 1.5 mM DTT. Each F$_n$Y$_{356}$−R2 was judged to be >95% pure on the basis of SDS−PAGE analysis. Each R2 was further characterized by ESI-MS, and the tyrosyl radical was quantitated by UV−vis and EPR spectroscopic methods (Table 3).

Purification of R1 and Removal of Contaminating R2. R1 (SA 1900 nmol/min/mg) was purified as previously described.[26] To reduce the redox-active cysteines of R1 and the Y• of contaminating R2, which copurifies with R1, R1 (~40 μM) was incubated with 30 mM DTT for 25 min at room temperature. Hydroxyurea, ATP, and CDP were

(25) Lapatsanis, L.; Milias, G.; Froussios, K.; Kolovos, M. *Synthesis* **1983**, 671.

(26) Salowe, S.; Bollinger, J. M., Jr.; Ator, M.; Stubbe, J.; McCraken, J.; Peisach, J.; Samano, M. C.; Robins, M. J. *Biochemistry* **1993**, *32*, 12749.

then added to final concentrations of 30, 3, and 1 mM, respectively, and the incubation was continued for an additional 20 min at room temperature. R1 was then isolated using a Sephadex G-25 column (~35 mL, 1.5 cm × 23 cm), which had been equilibrated in assay buffer (50 mM HEPES, 15 mM $MgSO_4$, 1 mM EDTA, pH 7.6).

Determination of pH Rate Profiles of F_nY_{356}−R2s. 2-[*N*-morpholino]ethanesulfonic acid (MES), *N*-2-hydroxyethylpiperazine-*N*-2-ethanesulfonic acid (HEPES), *N*-[Tris(hydroxymethyl)methyl]-3-aminopropanesulfonic acid (TAPS), and 2-[cyclohexylamino]ethanesulfonic acid (CHES) were used for the pH rate profiles. Each buffer was adjusted to the desired pH with either KOH or HCl. Each reaction contained in a volume of 230 μL: 50 mM HEPES (or MES, TAPS, CHES), 15 mM $MgSO_4$, 1 mM EDTA, 3 mM ATP, 1 mM [2-^{14}C]-CDP ($6 \times 10^6 - 1.5 \times 10^7$ cpm/μmol), 30 μM TR, 0.5 μM TRR, 1 mM NADPH, 3 μM R1, and 3 μM F_nY_{356}−R2. For each reaction, nucleotides, TR, TRR, and R1 were incubated at 25 °C for ~1.5−2 min. The reaction was then initiated by the addition of F_nY_{356}−R2 and NADPH. At defined time points, 40 μL were withdrawn and quenched with 25 μL of 2% perchloric acid. At the end of the time course, the reactions were neutralized with 20 μL of 0.5 M KOH. Each sample was incubated at −20 °C overnight to ensure complete precipitation of potassium perchlorate. The samples were then spun down for 3 min in a tabletop centrifuge. Each supernatant was transferred to a 1.5-mL screw-top microfuge tube, to which was added 14 units of calf-intestine alkaline phosphatase, 120 nmol of carrier deoxycytidine (dC), and Tris-EDTA buffer (pH 8.5) to a final concentration of 75 mM and 0.15 mM, respectively. The amount of dC was then quantitated by the method of Steeper and Steuart.[27]

Results

Synthesis and Characterization of $F_nY_{356}/V_{353}G/S_{354}C$−R2s. R2 is a homodimer containing 375 amino acids per monomer, which can be prepared semisynthetically by intein methods.[21] Residues 1−353 of R2 with its C-terminus fused to the *VmaI* intein and a chitin-binding domain were made via molecular biological methods. Residues 357−375 were synthesized by automated solid-phase peptide synthesis with residues 354, 355, and 356 being added in solution manually.[21−23] A number of minor changes have been made from our initially reported procedure to enhance recoveries of R2 and in efforts to increase the amount of Y• per R2. In general, C354 of the C-terminal tail of R2 can form a disulfide with the excess peptide used in the ligation reaction to generate full-length R2. Removal of the peptide is essential for accurate quantitation of RNR activity as the peptide is a competitive inhibitor of the nucleotide-reduction process.[28] The final purification steps, therefore, used concentration/dilution cycles to remove noncovalently bound peptide as well as anion exchange chromatographay on a MonoQ column with DTT in all the buffers to reduce the peptide−R2 disulfide bond and remove the peptide. Although DTT has previously been shown to reduce the Y• in R2,[29] the minimal time required for this purification step ensures that this side reaction does not occur. A summary of the recovery of semisynthetic R2s, their characterization by ESI-MS, the amount of Y• per R2, and the maximum specific activity of each R2, are presented in Table 3.

Over the past few years we have continually modified various aspects of the semisynthesis of R2 to improve yields and the amount of Y• recovered. We have performed all of the ligation reactions described here, with the exception of the 2,3-F_2Y-peptide, on the same batch of R2−thioester. As a control for all of our experiments, wt R2 made by the intein procedure (containing $V_{353}G/S_{354}C/Y_{356}$ and from here on referred to as Y−R2) was generated from the same batch and is reported in Table 3. Its specific activity is identical to the double mutant made by site-directed mutagenesis after normalization for the amount of Y•. The amount of Y• radical was quantified by X-band EPR spectroscopy and by the dropline correction method using the vis spectrum.[30,31]

Problems Encountered in the RNR Activity Assay. Because we wished to set lower limits of detection on the rates of deoxynucleotide formation with the mutant RNRs, we made two changes to the standard assays.[21] First, R1 (specific activity of 1.9 μmol/min/mg), as isolated, always copurifies with a small amount of R2 (estimated to be <1% by SDS PAGE). We therefore inactivated this contaminating R2 by reducing the tyrosyl radical with hydroxyurea in the presence of DTT, ATP, and CDP and showed, with control experiments in the absence of the R2 mutant, that no dNDP was detectable within the time frame of the assay. (Figure S1, Supporting Information). Second the peptide used to generate semisynthetic R2 is a known competitive inhibitor of the interaction of R2 with R1. An additional purification step for R2 mutants was thus added to the protocol to ensure that all of the peptide (covalently and noncovalently bound to R2) was removed. In each R2, there is now a cysteine at position 354 in place of the serine of the wt R2. R2 mutants containing this cysteine are inactivated in the presence of R1, CDP, and ATP in a slow, time-dependent reaction.[21] This inactivation presumably results from an uncoupling of the radical propagation pathway, resulting in the reduction of Y122•. Control experiments showed that this uncoupling did not occur to any significant extent under the conditions of the assays (Figure S2, Supporting Information). Finally, to ensure that the single amino acid substitution does not effect the interaction between the R1 and R2, the K_m values for several of the mutants were determined and found to be identical to Y−R2, as listed in Table 3.

pH Rate Profiles for wt and F_nY_{356}−R2s. Kinetic assays for nucleotide reduction over the RNR-accessible pH range from 6.5 to 9 were carried out to determine if direct evidence for the role of Y_{356} as a redox-active amino acid on a pathway between R1 and R2 could be obtained. The results of our kinetic assays for the various F_nY_{356}−R2s are shown in Figure 2 and are quite dramatic. First, all of the F_nY_{356}−R2s are active between pH 6.5 to 8.5, and the activity is relatively high despite the complexity of the semisynthetic procedure for R2 generation (Table 3). Second, the activities of 2,3-F_2Y_{356}−R2, 3,5-F_2Y_{356}−R2, and 2,3,5-F_3Y_{356}−R2 are very close to that of Y−R2 in the pH range from 6.5 to 7.6. On the alkaline side, the activity drops off for all F_nY derivatives with the dropoff beginning at a lower pH for the 2,3,5-F_3Y_{356}-, 2,3,6-F_3Y_{356}-, and 2,3,5,6-F_4Y_{356}−R2s. With 2,3,6-F_3Y_{356}−R2 and 2,3,5,6-F_4Y_{356}−R2, the activity relative to Y−R2 is substantially reduced throughout the entire pH rate profile. At pH values greater than 8.5, the activity is below the lower limit of detection of our assay method.

(27) Steeper, J. R.; Steuart, C. D. *Anal. Biochemistry* **1970**, *34*, 123.
(28) Climent, I.; Sjöberg, B. M.; Huang, C. Y. *Biochemistry* **1991**, *31*, 5164.
(29) Fontecave, M.; Gerez, C.; Mansuy, D.; Reichard, P. *J. Biol. Chem.* **1990**, *265*, 10919.
(30) Bollinger, J. M., Jr. Ph.D. Thesis, Massachusetts Institute of Technology, 1993.
(31) Bollinger, J. M., Jr.; Tong, W. H.; Ravi, N.; Huynh, B. H.; Edmondson, D. E.; Stubbe, J. *Methods Enzymol.* **1995**, *258*, 278.

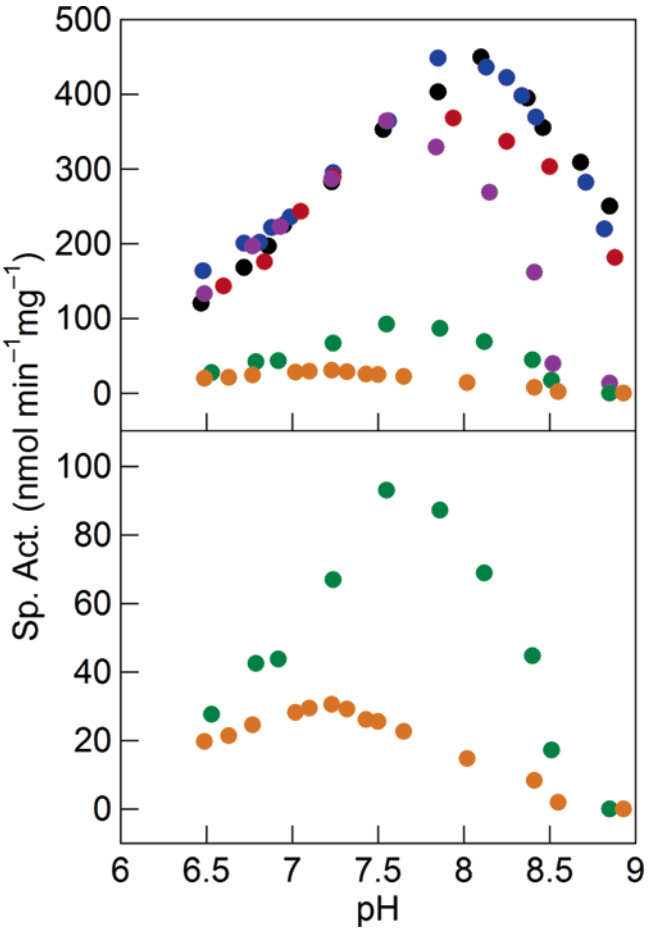

Figure 2. pH rate profiles of F_nY_{356}−R2s. The top panel shows an overlay of the pH rate profiles of Y−R2 and F_nY_{356}−R2s used in this study. (Bottom panel) Blowup of the profiles of 2,3,6-F_3Y_{356}−R2 and F_4Y_{356}−R2. Each point represents an average of two independent measurements. Error was within 15% for all points: (black ●) Y_{356}−R2, (blue ●) 3,5-F_2Y_{356}−R2, (red ●) 2,3-F_2Y_{356}−R2, (purple ●) 2,3,5-F_3Y_{356}−R2, (green ●) 2,3,6-F_3Y_{356}−R2, and (orange ●) F_4Y_{356}−R2.

Discussion

The F_nYs in Table 1 were incorporated into R2 by the intein procedure. They were chosen to perturb the protonation state and reduction potential of residue 356 in an effort to examine its role in the radical-propagation process. For each mutant R2, the ability to make deoxynucleotides was measured over the accessible pH range for RNR (6.5−9). The results, Figure 2, reveal that the F_nYs markedly perturb the activity, suggesting that these mutants will be useful for examining radical propagation.

The observed drop in RNR activity of F_nY−R2 mutants relative to Y−R2 may be related to changes in their reduction potentials. Unfortunately, one cannot measure the reduction potentials of these F_nYs within R2. We can, however, measure the peak-reduction potentials of Ac−F_nY−NH_2 derivatives. These values were determined in the pH range in which RNR activity can be measured (6.5−9, Figure 3) using differential pulse voltammetry (DPV).[24] Previous work has shown that the peak potential for the tyrosyl radical as measured by DPV is very similar to its reduction potential measured by cyclic voltammetry and pulse radiolysis.[32] The data in Figure 3 show

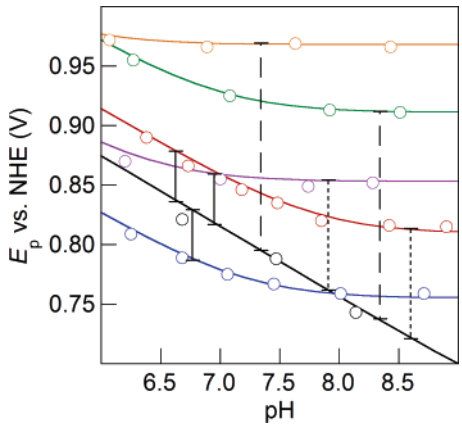

Figure 3. pH profiles of Ac−F_nY•−NH_2 peak-reduction potentials. The E_p vs pH for reduction of (black —) Ac−Y•−NH_2, (blue —) Ac−3,5-F_2Y•−NH_2, (red —) Ac−2,3-F_2Y•−NH_2, (purple —) Ac−2,3,5-F_3Y•−NH_2, (green —) Ac−2,3,6-F_3Y•−NH_2, and (orange —) Ac−F_4Y•−NH_2[24] in the pH range accessible to RNR are shown. Lines indicate peak-reduction potential differences of ±40 mV (solid), 90 mV (short dashes), and 180 mV (long dashes) relative to those for Ac−Y•−NH_2.

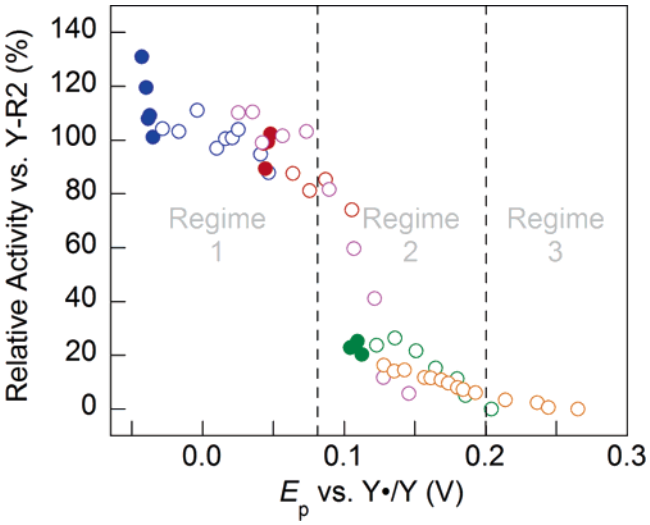

Figure 4. Redox-potential regimes of RNR activity. Relative activities of F_nY_{356}−R2s vs Y−R2, obtained from Figure 2, plotted as a function of the peak-reduction potential difference between the corresponding Ac−F_nY•−NH_2 and Ac−Y•−NH_2:[24] (blue ●,○) 3,5-F_2Y_{356}−R2, (red ●,○) 2,3-F_2Y_{356}−R2, (purple ○) 2,3,5-F_3Y_{356}−R2, (green ●,○) 2,3,6-F_3Y_{356}−R2, and (orange ○) F_4Y_{356}−R2. Filled circles represent data points where pH < pK_a of the corresponding F_nY; open circles represent data points where pH > pK_a of the corresponding F_nY. Three different regimes of RNR activity are highlighted as either gated by a physical/conformational change (regime 1), rate limited by radical transport (regime 2), or reduced to background levels (regime 3), depending on the peak-reduction potential difference between the corresponding Ac−F_nY•−NH_2 and Ac−Y•−NH_2.

that the fluorinated tyrosine derivatives have potentials that vary from −50 to +270 mV relative to tyrosine.

To gain insight into the relationship between RNR activity and the reduction potential of residue 356, Figure 4 was generated. In this Figure, the activity data of each mutant relative to that of Y−R2 is plotted against the peak-reduction potential difference between Ac−F_nY−NH_2 and Ac−Y−NH_2. Analysis of the data in this fashion allows for the removal of the pH-dependent activity inherent to Y−R2 and assumes that all of the mutants have the same inherent pH dependence. The basis of this pH dependence is not understood. The construction of Figure 4 also assumes that the reduction potential of Y_{356}• and

(32) Tommos, C.; Skalicky, J. J.; Pilloud, D. L.; Wand, A. J.; Dutton, P. L. *Biochemistry* **1999**, *38*, 9495.

F_nY_{356}• varies 59 mV/pH unit, as with E_p(Ac−F_nY•−NH_2/Ac−F_nY−NH_2) and requires proton loss to bulk solution concomitant with oxidation. Furthermore, we assume that if the protein environment perturbs the reduction potential for Y in Y−R2, it has the same relative effect on each F_nY in the corresponding F_nY_{356}−R2. We note that the data in Figure 4 reveal some scatter, which we attribute in part to the difficulties with making R2 semisynthetically. Moreover, fluorine substitution may affect the conformation of residue 356 and its interactions with its environment. Four fluorines certainly have altered steric properties relative to four hydrogens, stemming from the slightly larger van der Waals radius of F vs H (1.35 vs 1.2 Å, respectively) and the longer C−F bond vs the C−H bond (1.38 and 1.09 Å, respectively). Finally, using the pK_a of Ac−F_nY−NH_2 as a benchmark for F_nY_{356}, a difference in charge of this residue may result owing to the pK_a differences of each of these fluorinated tyrosines. Given the incongruities that may be engendered by fluorine substitution, the data in Figure 4 are quite striking.

Three distinct activity regimes emerge from Figure 4. When peak-reduction potential differences are −50 to 80 mV (regime 1), nucleotide-reduction activity falls within the range of that observed for Y−R2; both 2,3-F_2Y_{356}−R2 and 3,5-F_2Y_{356}−R2 exhibit 90−120% of the activity obtained for Y−R2. As the difference in peak-reduction potential increases from 80 to 200 mV (regime 2), the RNR activity drops off dramatically. At >200 mV difference (regime 3), no detectable activity of RNR is observed. 2,3,5-F_3Y_{356}−R2 spans the potential range from ∼25 to 145 mV, whereas 2,3,6-F_3Y_{356}−R2 and F_4Y_{356}−R2 have very low activities and high peak-reduction potential differences at all pHs accessible to RNR.

Our interpretation of these data is summarized by the three activity regimes marked with dashed lines in Figure 4. When the reduction potential difference is within the range of −50 to 80 mV (regime 1), the rate of nucleotide reduction in the F_nY_{356}−R2s is governed by the same factors as nucleotide reduction by Y−R2. Presteady-state experiments have shown that the rate-limiting step in *E. coli* RNR is a physical step or steps prior to the radical propagation process that is gated by the binding of a substrate and allosteric effector.[13] In the steady state, the rate-determining step is proposed to be the same physical step or, alternatively, a step involved in rereduction of R1 or a conformational change associated with this rereduction, after dNDP formation and regeneration of the Y•.[21] In either case, the rate of nucleotide reduction should be independent of the Y_{356}•-reduction potential, leading us to assign regime 1 to the physically/conformationally gated step. The peak-reduction potential of Ac−3,5-F_2Y•−NH_2 falls effectively in the conformationally gated regime over all pHs, whereas the potentials of Ac−2,3-F_2Y•−NH_2 and Ac−2,3,5-F_3Y•−NH_2 falls within this regime for pH <∼8.4 and pH ≤∼7.6, respectively. At a pH of 6.81 (solid line, Figure 3), the peak-reduction potential difference between Ac−3,5-F_2Y•−NH_2 and Ac−Y•−NH_2 is −40 mV. Similarly, at pHs of 6.6 and 6.93 (solid lines, Figure 3), the peak-reduction potentials of Ac−2,3-F_2Y•−NH_2 and Ac−2,3,5-F_3Y•−NH_2, respectively, are ∼40 mV higher than that of Ac−Y•−NH_2. The relative activities are all identical within error (108, 99, and 100% of Y−R2, respectively, for 3,5-F_2Y_{356}−R2, 2,3-F_2Y_{356}−R2, and 2,3,5-F_3Y_{356}−R2).

When the driving force for Y_{356} oxidation exceeds 80 mV but is less than 200 mV relative to Y, the rate of nucleotide reduction correlates with the difference in peak-reduction potential, suggesting that there has been a change in the rate-limiting step to one involving radical transport through F_nY_{356}. This point is demonstrated for 2,3-F_2Y_{356}−R2 and 2,3,5-F_3Y_{356}−R2. The short dashed lines in Figure 3 indicate two pH values (8.6 and 7.8) at which the peak-reduction potential difference between Ac−2,3-F_2Y•−NH_2 and Ac−Y•−NH_2 and between Ac−2,3,5-F_3Y•−NH_2 and Ac−Y•−NH_2 is ∼90 mV. If activity is determined solely by the reduction potential, then the relative activity of 2,3-F_2Y_{356}−R2 at pH 8.5 should approximate that of 2,3,5-F_3Y_{356}−R2 at pH 7.8. The relative activities observed are 85% and 81%, respectively.

At potential differences greater than 150 mV (regime 3), the rate of radical transfer appears to become so slow that nucleotide reduction is minimal, and for potential differences >200 mV, activity is abolished. Note that the relative activities of 2,3,6-F_3Y_{356}−R2 at pH 8.4 and of F_4Y_{356}−R2 at pH 7.4, where the peak-reduction potential difference between these corresponding Ac−F_nY•−NH_2s and Ac−Y•−NH_2 is 180 mV (long dashed lines, Figure 3), are 11% and 8%, respectively. The direct correlation between activity and peak-reduction potential strongly suggests that Y_{356} is a redox-active amino acid on the pathway.

We also examined whether the protonation state of the F_nYs at position 356 affects RNR activity. Our previous studies with NO_2Y_{356}−R2[21] showed that the pK_a of this residue at the R1/R2 interface is unperturbed relative to that of Ac−NO_2Y−NH_2 in solution. Similar measurements of the pK_as of the F_nYs within R2 cannot be made because these phenolates do not absorb in the visible region of the spectrum as does 3-NO_2Y^-. We have thus assumed that the pK_as of the Ac−F_nY−NH_2 are indicative of those within the R1/R2 complex. We have incorporated this information into Figure 4 in an effort to determine if the protonation state of F_nY has any correlation with RNR activity: Filled circles in Figure 4 represent data points where pH < pK_a of the corresponding F_nY; conversely, open circles represent data points where pH > pK_a of the corresponding F_nY. This analysis reveals that most of the F_nYs used in this study are deprotonated or exhibit changes in protonation state, whereas Y, because of its higher pK_a, remains protonated throughout the range where the activity of RNR can be measured. In contrast with the peak-potential data, no clear correlation exists between the protonation state of the F_nY_{356} and the activity of the corresponding mutant.

Our results do not provide any insight about the destination of the proton from Y_{356} in Y−R2 in the forward PCET event or its delivery in the back PCET event. A comparison of the sequences of the disordered C-terminal tails of >160 R2s suggests that, although there are no absolutely conserved residues, E_{350} is present in 129 of 162 R2 sequences.[33] Thus, it is possible that this residue functions as a proton acceptor in the forward PCET reaction and a proton donor in the reverse reaction. The importance of this residue is supported by mutagenesis studies carried out on many of the residues within the C-terminus of R2. Individual substitution of Y_{356} and E_{350} with alanine was found to affect activity. In the former case, R2 was inactive, and in the latter case, the rate was reduced 250-fold.[34]

(33) Ge, J. Ph.D. Thesis, Massachusetts Institute of Technology, 2003.

The mechanistic details for radical transport involving a tyrosyl radical at this position are important to consider. Radical transport involving the deprotonated fluorotyrosines can proceed by simple ET (eq 1). Conversely, a stepwise ET/PT reaction of a protonated tyrosine confronts a large thermochemical bias because $\Delta G°$ for the initial ET or PT event is high.[35−38] Accordingly, these thermodynamic constraints implicate proton-coupled electron transfer (PCET) for radical propagation (eq 2).[39−42]

$$F_nY\bullet + e^- \rightarrow F_nYO^- \quad (1)$$

$$Y\bullet + e^- + H^+ \rightarrow YOH \quad (2)$$

In Y−R2, therefore, the proton must be lost concomitant with Y_{356} oxidation via PCET.

Assuming the radical-propagation pathway shown in Figure 1, our results with the F_nY_{356}−R2s suggest that hole migration between the W_{48}−R2−Y_{356}−R2 pair and the Y_{356}−R2−Y_{731}−R1 does not occur by an obligatory hydrogen atom transfer as phenolates of the F_nY_{356}−R2s are active. Furthermore, this activity for the phenolates is inconsistent with the models based on site-directed mutagenesis studies[15] and the theory[43] that W_{48}, Y_{356}, and Y_{731} are connected by way of a hydrogen-bonding network that is required for conformational gating of the radical-propagation process. The turnover number of 2,3,5-F_3Y_{356}−R2 at pH 7.6, for example, is identical to that of Y−R2, where it is deprotonated if one assumes that the pK_a is not perturbed from that of Ac−2,3,5-F_3Y−NH_2, as indicated by our studies on NO_2Y_{356}−R2.[21] W_{48} and Y_{731} must, therefore, communicate by ET involving the 2,3,5-F_3Y^-/2,3,5-F_3Y• couple. The insertion of a negative charge at the R1/R2 interface apparently does not affect the overall RNR activity. These results, taken together with our preliminary studies,[22,23] lead us to conclude that the proton from Y_{356} in the wt enzyme is transferred (off pathway) to solvent, either directly or via a base or bases in R2 or R1.

Conclusions

A major unresolved issue in class I RNRs is the mechanism of radical propagation—how does Y_{122}• on R2, transiently and reversibly, generate a C_{439}• on R1 proposed to be >35 Å away? This problem is different from most ET reactions in biology studied to date, which typically occur over a distances of 10−15 Å by a tunneling mechanism and, consequently, do not involve aromatic amino acid radical intermediates.[44−56] The participation of tyrosine in the radical-initiation pathway of RNR steps beyond simple ET because the management of proton and electron inventories is required for charge transport involving the amino acid. In the accompanying paper, we have shown that fluorotyrosine derivatives have radical peak-reduction potentials from −50 to +270 mV relative to Y and pK_as that range from 5.6 to 7.8. By exploiting these properties for F_nYs substituted at Y_{356}, our data strongly suggest that this residue in R2 is a redox-active amino acid on the radical-propagation pathway in the class I RNRs. This result is important as Y_{356} is the only residue on the pathway that is not observable structurally. Different activity regimes of RNR may be accessed by tuning the reduction potential of F_nY_{356}• such that radical transport becomes rate limiting in nucleotide reduction. Future experiments using presteady-state kinetic analyses will focus on establishing that the radical-propagation process does, in fact, become rate limiting at peak-reduction potential differences >80 mV, as proposed on the basis of our reported data, as well as on detection of radical amino acid intermediates during turnover. Studies reported herein further strongly suggest that hole migration between the W_{48}−R2−Y_{356}−R2 pair and the Y_{356}−R2−Y_{731}−R1 does not occur by a hydrogen-atom transfer, as phenolates of the F_nY_{356}−R2s are active. The obligation of protons to the pathway from Y_{122} to Y_{356} in R2 and from Y_{731} into C_{439} at the active site of R1 remains an open question and needs to be investigated, most efficiently by direct kinetic analysis of the radical intermediates. These studies are currently underway.

Acknowledgment. We thank John H. Robblee for help with the quantitation of radical per R2 dimer via EPR and for helpful discussions and the National Institutes of Health for support of this work GM47274 (D.G.N.) and GM29595 (J.S.).

Supporting Information Available: Solvent systems and R_f values for purification of the Fmoc-F_nYs (Table S1); background activity assay on prereduced R1 (Figure S1); control experiments for uncoupling (Figure S2). This material is available free of charge via the Internet at http://pubs.acs.org.

JA055927J

(34) Climent, I.; Sjöberg, B. M.; Huang, C. Y. *Biochemistry* **1992**, *31*, 4801.
(35) Mayer, J. M.; Rhile, I. J. *Biochim. Biophys. Acta* **2004**, *1655*, 51.
(36) Sjödin, M.; Ghanem, R.; Polivka, T.; Pan, J.; Styring, S.; Sun, L.; Sundström, V.; Hammarström, L. *Phys. Chem. Chem. Phys.* **2004**, *6*, 4851.
(37) Sjödin, M.; Styring, S.; Wolpher, H.; Xu, Y.; Sun, L.; Hammarström, L. *J. Am. Chem. Soc.* **2005**, *127*, 3855.
(38) Reece, S. Y.; Nocera, D. G. *J. Am. Chem. Soc.* **2005**, *127*, 9448.
(39) Chang, C. J.; Chang, M. C. Y.; Damrauer, N. H.; Nocera, D. G. *Biochim. Biophys. Acta* **2004**, *1655*, 13.
(40) Cukier, R. I.; Nocera, D. G. *Annu. Rev. Phys. Chem.* **1998**, *49*, 337.
(41) Cukier, R. I. *Biochim. Biophys. Acta* **2004**, *1655*, 37.
(42) Hatcher, E.; Soudackov, A. V.; Hammes-Schiffer, S. *J. Am. Chem. Soc.* **2004**, *126*, 5763.
(43) Himo, F.; Siegbahn, P. E. M. *Chem. Rev.* **2003**, *103*, 2421.
(44) Page, C. C.; Moser, C. C.; Chen, X.; Dutton, P. L. *Nature* **1999**, *402*, 47.
(45) *Electron Transfer in Chemistry*; Balzani, V., Ed.; Wiley-VCH: Weinheim, Germany, 2001; Vol. 3, Part 1.
(46) Gray, H. B.; Winkler, J. R. *Annu. Rev. Biochem.* **1996**, *65*, 537.
(47) Gunner, M. R.; Robertson, D. E.; Dutton, P. L. *J. Phys. Chem.* **1986**, *90*, 3783.
(48) Farver, O.; Pecht, I. *Biophys. Chem.* **1994**, *50*, 203.
(49) Namslauer, A.; Braenden, M.; Brzezinski, P. *Biochemistry* **2002**, *41*, 10369.
(50) Tollin, G. In *Electron Transfer in Chemistry*; Balzani, V., Ed.; Wiley-VCH: Weinheim, Germany, 2001; Vol. 4, Part 1, p 202.
(51) Davidson, V. L. *Acc. Chem. Res.* **2000**, *33*, 87.
(52) McLendon, G.; Hake, R. *Chem. Rev.* **1992**, *92*, 481.
(53) Millett, F.; Durham, B. *Biochemistry* **2002**, *41*, 11315.
(54) Nocek, J. M.; Zhou, J. S.; Forest, S. D.; Priyadarshy, S.; Beratan, D. N.; Onuchic, J. N.; Hoffman, B. M. *Chem. Rev.* **1996**, *96*, 2459.
(55) Lewis, F. D. Electron Transfer and Charge Transport in DNA. In *Electron Transfer in Chemistry*; Balzani, V., Ed.; Wiley-VCH: Weinheim, Germany, 2001; Vol. 3, Part 5, p 105.
(56) Boon, E. M.; Barton, J. K. *Curr. Opin. Struct. Biol.* **2002**, *12*, 320.